Mechanistic Studies of the Flavoenzyme Tryptophan 2-Monooxygenase: Deuterium and ^{15}N Kinetic Isotope Effects on Alanine Oxidation by an L-Amino Acid Oxidase[†]

Erik C. Ralph,[‡] Mark A. Anderson,[§] W. Wallace Cleland,[§] and Paul F. Fitzpatrick*,[‡,#]

Departments of Biochemistry and Biophysics and of Chemistry, Texas A&M University, College Station, Texas 77843-2128 and Institute for Enzyme Research and Department of Biochemistry, University of Wisconsin, Madison, Wisconsin 53726

ABSTRACT: Tryptophan 2-monooxygenase (TMO) from *Pseudomonas savastanoi* catalyzes the oxidative decarboxylation of L-tryptophan during the biosynthesis of indoleacetic acid. Structurally and mechanistically, the enzyme is a member of the family of L-amino acid oxidases. Deuterium and ^{15}N kinetic isotope effects were used to probe the chemical mechanism of L-alanine oxidation by TMO. The primary deuterium kinetic isotope effect was pH independent over the pH range 6.5−10, with an average value of 6.0 ± 0.5, consistent with this being the intrinsic value. The deuterium isotope effect on the rate constant for flavin reduction by alanine was 6.3 ± 0.9; no intermediate flavin species were observed during flavin reduction. The k_{cat}/K_{ala} value was 1.0145 ± 0.0007 at pH 8. NMR analyses gave an equilibrium ^{15}N isotope effect for deprotonation of the alanine amino group of 1.0233 ± 0.0004, allowing calculation of the ^{15}N isotope effect on the CH bond cleavage step of 0.9917 ± 0.0006. The results are consistent with TMO oxidation of alanine occurring through a hydride transfer mechanism.

The flavoenzyme tryptophan 2-monooxygenase (TMO)[1] from *Pseudomonas savastanoi* catalyzes the oxidative decarboxylation of L-tryptophan (Scheme 1) in the first step of a two-step biosynthetic pathway for the plant hormone indoleacetic acid (*10−12*). The kinetic mechanism of TMO has been determined with its fastest substrate L-tryptophan (*13*) and can be divided into two half-reactions (Scheme 2). The reductive half-reaction involves cleavage of the α-CH bond of the amino acid (AA) and transfer of a hydride equivalent to the FAD to form the enzyme-bound imino acid. This is identical to the reaction of the flavoprotein L-amino acid oxidases and similar to the general reaction of flavoprotein amine oxidases. In the oxidative half-reaction of TMO, the reduced cofactor reacts with oxygen to produce hydrogen peroxide (*14*). Decarboxylation of the imino acid to the amide is thought to occur through the reaction of the hydrogen peroxide with the imino acid still bound to the enzyme (pathway a), analogously to the mechanism proposed by Lockridge et al. (*15*) for the decarboxylation of pyruvate by lactate oxidase. Although indoleacetamide is the only product of tryptophan turnover by wild-type TMO, amino acid oxidation can be uncoupled from decarboxylation to yield a keto acid in mutant enzymes (pathway b) (*16, 17*).

Scheme 1
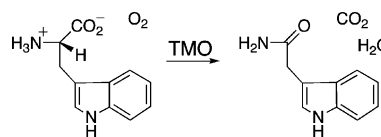
Scheme 2
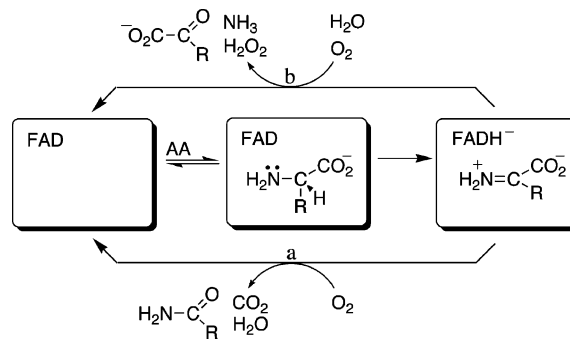
Despite their ubiquity and functional diversity, all flavin-dependent amine oxidases have thus far fallen into two structural families. One family includes D-amino acid oxidase (*18*), monomeric sarcosine oxidase (*19*), and glycine oxidase (*20*), while monoamine oxidase (*21*), polyamine oxidase (*22*), and L-amino acid oxidase (*23*) represent a separate family. Although the three-dimensional structure of TMO has not been determined, sequence analyses (*24*) and site-directed mutageneses (*16, 17*) have established that the enzyme is structurally an L-amino acid oxidase.

Despite a number of biochemical and kinetic studies, the mechanism of amine oxidation by flavoenzymes is still heavily debated. The commonly proposed mechanisms for the oxidation of primary amines (for recent reviews see refs *25* and *26*) are represented in Schemes 3−5, with alanine

---

* Address correspondence to Department of Biochemistry and Biophysics 2128 TAMU College Station, Texas 77843-2128. Ph: 979-845-5487. Fax: 979-845-4946. E-mail: fitzpat@tamu.edu.
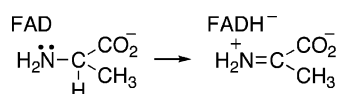[‡] Department of Biochemistry and Biophysics, Texas A&M University.
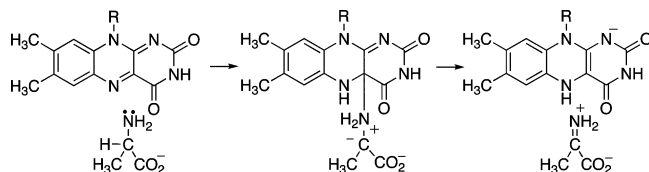[#] Department of Chemistry, Texas A&M University.
[§] University of Wisconsin.
[1] Abbreviations: TMO, tryptophan 2-monooxygenase from *Pseudomonas savastanoi*; IRMS, isotope ratio mass spectrometry.
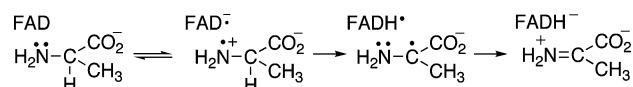
Scheme 3

Scheme 4

Scheme 5

as substrate. The simplest mechanism for amine oxidation, shown in Scheme 3, involves a direct hydride transfer from the substrate α-C to the flavin. The mechanism of Scheme 4 involves a nucleophilic attack of the substrate nitrogen on the flavin cofactor, resulting in a covalent flavin-alanine intermediate that cleaves to form the products. Scheme 5 involves the formation of a flavin-substrate radical pair, which could then be resolved through either separate proton and electron transfers as shown or through a hydrogen atom transfer from the substrate α-carbon.

With the exception of a direct hydride transfer, each of the postulated mechanisms utilizes an intermediate flavin species between fully oxidized and fully reduced flavin. To date, there is no spectroscopic evidence for an intermediate flavin species in TMO. However, CH bond cleavage is not fully rate-limiting with any of the well-characterized substrates. It is therefore not unreasonable that formation of an intermediate flavin species may occur during or subsequent to a rate-limiting step, thereby preventing its detection. In the present study, we characterize TMO turnover of L-alanine. pH studies and primary deuterium and ^{15}N kinetic isotope effects were used to identify the rate-limiting step and to evaluate the chemical mechanism. The results suggest that TMO utilizes a hydride transfer mechanism.

EXPERIMENTAL PROCEDURES

Materials. DL-α^2H-Alanine was purchased from Cambridge Isotope Laboratories, Inc. (Andover, MA) and MSD Isotopes (Montreal, Canada). ^{15}N-Phenylalanine, ^{15}N-alanine, and ^{15}N-glycine were from Sigma-Aldrich. The HiPrep DEAE column was from Amersham Pharmacia Biotech (Uppsala, Sweden).

Protein Expression and Purification. TMO was expressed in M15 *Escherichia coli* (pREP4) using a pQE51-based plasmid as previously described (*16*). Methods for enzyme purification were based on those previously described (*27*), with several modifications. Cells harvested from 9 L of culture were resuspended in 100 mL of 0.1 M Tris, 12 mM β-mercaptoethanol, 50 μM indoleacetamide, 1 mM EDTA, 1 mM phenylmethylsulfonyl fluoride, 100 μg mL^{-1} lysozyme, pH 8.3, and lysed with a Branson Sonifier 450 for three 6-min intervals at 30% output. The clarified lysate was prepared by centrifugation and treated with polyethylene-

imine as previously described (*27*). The resulting supernatant was made 20% saturated in ammonium sulfate, precipitated via centrifugation, and the precipitate discarded. The supernatant was made 60% saturated in ammonium sulfate and precipitated as before. The resulting pellet was resuspended in 10−15 mL of 0.1 M Tris, 50 μM indoleacetamide, 1 mM EDTA, 1 mM dithiothreitol, pH 8.3, and dialyzed overnight against two changes of 50−100 vol of the same buffer. Denatured protein was removed by centrifugation. The protein sample was purified in two portions using a 20 mL HiPrep 16/10 DEAE Fast Flow column. The column was equilibrated with 0.1 M Tris, 50 μM indoleacetamide, pH 8.3, loaded with a protein sample, and subsequently washed with 20 mL of equilibration buffer. Protein was eluted with a 400 mL linear gradient of 0−125 mM potassium chloride in 0.1 M Tris, 50 μM indoleacetamide, pH 8.3. To regenerate the column, it was washed with 20 mL of 2 M sodium chloride, 10 mL of 1 M sodium hydroxide, and 50 mL of water, and then re-equilibrated with the starting buffer. The eluted fractions were analyzed for protein and flavin content, based on absorbance values at 280 and 466 nm, respectively. Fractions with the greatest flavin to protein ratio were pooled and precipitated with 60% saturated ammonium sulfate. The purified enzyme was resuspended to a final concentration of 300−500 μM in 10 mM potassium pyrophosphate, 10% glycerol, pH 8.3.

Removal of Bound 3-Indoleacetamide. Bound indoleacetamide was removed as previously described (*27*), with the modification that EDTA was omitted from dialysis buffers and 10 mM potassium pyrophosphate was used in place of 0.1 M Tris-HCl to avoid nitrogen-containing buffers.

Enzyme Assays. Enzyme concentrations were calculated from the absorbance at 466 nm using the previously determined extinction coefficient of 11.4 mM^{-1} cm^{-1} (*27*). The rate of oxygen consumption was measured using a Hansatech oxygen-monitoring system (Norfolk, UK) with a computer-interfaced graphical mode or a Yellow Springs Instrument model 5300 oxygen electrode (Yellow Springs, OH). Steady-state kinetic parameters were routinely determined at 25 °C under atmospheric oxygen concentrations. When necessary, the oxygen concentration was varied by bubbling the desired oxygen/argon mixture through a reaction sample in the oxygen electrode cuvette until a constant oxygen concentration was observed. The reaction was then started by the addition of enzyme. To determine the amount of hydrogen peroxide formed, reactions were run in the presence and in the absence of 170 μg mL^{-1} catalase. Flavin reduction was monitored using a Hewlett-Packard 8452A photodiode array spectrophotometer. Substrates were prepared in 50 mM Tris, 5 mM D-glucose, pH 8.3 and made anaerobic by bubbling argon through 1 mL of solution for 15 min, prior to the addition of glucose oxidase (20 μg). A small volume of enzyme (50 μL) was placed in an anaerobic cuvette sealed with a rubber septum. The cuvette was made anaerobic by cycling between vacuum and argon. The reaction was started by injecting the substrate solution through the rubber septum.

^{15}N Kinetic Isotope Effects. ^{15}N Kinetic isotope effects were determined competitively using the natural abundance of ^{15}N and ^{14}N in L-alanine. Conditions were typically 0.3 M L-alanine, 0.3 M hydroxylamine, 20 mM potassium pyrophosphate, 100 μg mL^{-1} catalase, 10% glycerol, pH 8.0,

in 3−5 mL. The sample pH slowly decreased as the reaction progressed. Therefore, the pH was frequently monitored and adjusted with potassium hydroxide as necessary to keep the reaction samples within 0.1 pH units of the desired value. Additional TMO was added periodically to keep the reaction progressing. Reactions were stirred in the dark at 25 °C with wet 100% oxygen blowing over the surface. Reaction progress was monitored using a Waters Delta 600 HPLC with a model 2487 Dual λ Absorbance Detector. A 100 μL sample was withdrawn and mixed with 500 μL of 2.5 mM potassium phosphate in 70% MeCN, to give a pH reading of 8.0 (pH*). Protein was removed by either filtering the sample through a 0.20 μm nylon filter or by centrifugation for 20 min at 21000g. The sample was then loaded onto a Waters μBondapak-NH$_2$ column (3.9 × 300 mm) with a 100 μL loop and eluted isocratically with 2.5 mM potassium phosphate in 80% MeCN, pH* 8.0, at 3 mL min^{-1}. Alanine and pyruvate were detected by monitoring the absorbance at 210 and 250 nm, respectively. The fractional conversion of alanine to pyruvate was determined by comparing the peak areas of alanine and pyruvate to standard curves prepared using commercially available compounds.

After 25−45% of the alanine had been oxidized, reactions were quenched by the addition of 0.1 vol of concentrated hydrochloric acid. Protein was then removed by centrifugation. To remove free FAD, the sample was diluted to approximately 10 mg mL^{-1} alanine using 5 mM ammonium acetate and adjusted to pH 4 using potassium hydroxide; aliquots (1 mL) were loaded onto a Waters NovaPak C$_{18}$ column (3.9 × 150 mm). The alanine and pyruvate eluted together within 10 min with 5 mM aqueous ammonium acetate as the mobile phase at 1 mL min^{-1}. The FAD was then eluted with a 10 mL gradient of 5 mM ammonium acetate in 0−50% methanol. The eluate containing alanine and pyruvate was collected, pooled, and dried on a roto-evaporator. The dried sample was resuspended in 10 mL of approximately 1.3 mM potassium hydroxide and redried; this process was repeated three times to drive off ammonia.

Alanine and pyruvate were separated using a preparative Waters μBondapak-NH$_2$ column (7.8 × 300 mm). Dried samples were resuspended in water and acetonitrile to yield approximately 10 mg mL^{-1} alanine in 40−50% acetonitrile. The pH was adjusted to pH* 7. Samples (1 mL) were loaded onto the column and eluted at 4 mL min^{-1} with 80% MeCN, 2.5 mM potassium phosphate, pH* 7.5, while collecting 8 mL fractions. Alanine elutes around 25 min. The alanine fractions were pooled, dried on a rotary evaporator, resuspended in water, and lyophilized.

For isotope ratio mass spectrometry (IRMS) analysis, the alanine samples were combusted to produce nitrogen gas. Quartz tubes (0.9 cm o.d. × 0.7 cm i.d. × 24 cm long) were charged with 8−10 mg of alanine, 100 mg of diatomaceous earth, 3−4 g of cupric oxide, and 500 mg of elemental copper. The tubes were placed under vacuum, flame-sealed, and combusted at 850 °C. The nitrogen gas produced was distilled on a high vacuum line through two −78 °C traps and one −196 °C trap, and then trapped on molecular sieves at −196 °C. The isotopic composition of the gas was determined using a Finnegan delta E isotope ratio mass spectrometer.

The ^{15}N equilibrium isotope effects for deprotonation of the amino acids glycine, alanine, and phenylalanine were

measured by ^{13}C NMR using the method described by Rabenstein and Mariappan (*28*) with a few modifications. Solutions containing approximately 50 mg mL^{-1} glycine or alanine or 25 mg mL^{-1} phenylalanine were prepared in water and adjusted with potassium hydroxide to the desired pH. 50 μL of D$_2$O and 10 μL of 1,4-dioxane were added to 1 mL of amino acid solution. Spectra were collected at ambient temperature at 125.7 MHz and normalized for the chemical shift of the 1,4-dioxane. The equation defining the observed difference in chemical shifts of the ^{14}N- and ^{15}N-labeled amino acids as a function of the fractional concentration of the protonated form of the ^{14}N compound [defined as *n* in Rabenstein's eq 3 (*28*)] was expanded to include the relationship $n = (\delta_{obs} - \delta_d)/(\delta_p - \delta_d)$, where δ_{obs}, δ_d, and δ_p are the observed chemical shift for the ^{14}N-labeled compound, and the limiting values for this chemical shift at the high and low pH extremes, respectively. This allowed for the difference in chemical shifts of the ^{14}N- and ^{15}N-labeled compounds to be fit directly as a function of the observed chemical shift of the ^{14}N compound using eq 5 (see *Data analysis* below), thereby eliminating any error associated with the determination of the sample pH.

Data Analysis. The kinetic data were analyzed using the programs KaleidaGraph (Synergy Software, Reading, PA), Igor (Wavemetrics, Lake Oswego, OR), and SPECFIT (Spectrum Software Associates, Marlborough, MA). When the concentration of only one substrate was varied, the initial rates of oxygen consumption were fit to the Michaelis−Menten equation. The k_{cat}/K_{ala} values determined at different pH were fit to eq 1, where *H* is the concentration of the hydronium ion. Equation 1 describes a profile in which deprotonation of one ionizable group with pK_2 is essential for activity, deprotonation of a second group with pK_1 increases the activity, and deprotonation of a third group with pK_3 results in a loss of activity. This profile has two plateau regions defined by the term C_I and the sum of C_I and C_H. Deuterium kinetic isotope effects were obtained from fits of the data to eq 2, which describes equal isotope effects on k_{cat} and k_{cat}/K_{ala}; v/e is the initial rate of oxygen consumption divided by the enzyme concentration, F_i is the fraction of the heavy atom, and E_{KIE} is the isotope effect. The rates of flavin reduction under anaerobic conditions were determined from fits of the data to eq 3, which describes a monophasic exponential decay; *k* is the first-order rate constant, A_t is the absorbance at time *t*, and A_∞ is the final absorbance. The observed ^{15}N kinetic isotope effect (E_{obs}) was calculated using eq 4,[2] where *f* is the final fraction of alanine oxidized, and R_S/R_0 is the ^{15}N/^{14}N ratio of the alanine remaining after enzymatic oxidation divided by the ^{15}N/^{14}N ratio of the alanine prior to oxidation. The ^{15}N equilibrium isotope effect

---

[2] The derivation of eq 4 is shown below, starting with the equation more commonly used for secondary heavy atom isotope effects (*1*); E_{obs} is the observed ^{15}N isotope effect on k_{cat}/K_m, *f* is the final fraction of alanine oxidized, and R_S/R_0 is the ^{14}N/^{15}N ratio of the alanine after oxidation divided by the isotope ratio of the alanine prior to any enzymatic oxidation.

$$E_{obs} = \log(1 - f)/\log[(1 - f)(R_S/R_0)]$$

$$\log[(1 - f)*R_S/R_0] = [\log(1 - f)]/E_{obs}$$

$$(1 - f)*R_S/R_0 = (1 - f)^{(1/E_{obs})}$$

$$R_S/R_0 = (1 - f)^{(1/E_{obs})-1}$$

on alanine deprotonation was obtained by fitting the data to eq 5, which defines the difference in the chemical shifts of the ^{14}N and ^{15}N-labeled compounds ($\Delta_{14\text{-}15}$) as a function of the chemical shift of the ^{14}N compound; $^{15}K_{eq}$ is the equilibrium isotope effect and δ_{obs}, δ_d, and δ_p are the observed chemical shift for the ^{14}N-labeled compound and the limiting values for this chemical shift at the high and low pH extremes, respectively. The observed ^{15}N isotope effect on k_{cat}/K_m was corrected for the protonation state of the free substrate using eq 6, where $^{15}k_{chem}$ is the pH-independent isotope effect on k_{cat}/K_m, $^{15}K_{eq}$ is the equilibrium effect for alanine deprotonation, and 9.87 is the pK_a value of the alanine amine (*29*).

$$\log\left(\frac{k_{cat}}{K_m}\right) = \log\left[\frac{C_I + C_H/(1 + H/K_1)}{1 + H/K_2 + K_3/H}\right] \quad (1)$$

$$v/e = \frac{k_{cat}A}{(K_m + A)(1 - F_i + E_{KIE}F_i)} \quad (2)$$

$$A_{total} = A_t e^{-kt} + A_\infty \quad (3)$$

$$R_S/R_0 = (1 - f)^{(1/E_{obs}-1)} \quad (4)$$

$$\Delta_{14-15} = \frac{{}^{15}K_{eq}(\delta_{obs} - \delta_p)(\delta_d - \delta_p)}{({}^{15}K_{eq} - 1)(\delta_{obs} - \delta_p) + (\delta_d - \delta_p)} - (\delta_{obs} - \delta_p) \quad (5)$$

$$^{15}k_{chem} = \frac{E_{obs}}{1 + [({}^{15}K_{eq} - 1)/(1 + 10^{pH-9.87})]} \quad (6)$$

RESULTS

Steady-State Kinetics. The use of slow substrates is often beneficial in the study of enzyme mechanisms, as it increases the chances that chemical steps rather than substrate binding or product release will be rate-limiting. This allows for the direct measurement of intrinsic rate constants and isotope effects under steady-state conditions (*30*). L-Alanine was previously identified as a slow substrate for TMO (*13*). Consequently, alanine was further characterized as a substrate for TMO.

To determine the oxygen dependence of alanine turnover, initial rates of oxygen consumption were measured at 0.1 and 1.0 M L-alanine while varying the oxygen concentration from 50 to 425 μM. All assays were done at 25 °C in 50 mM Tris, pH 8.3, varying the potassium chloride concentration to maintain a constant ionic strength of approximately 1 M. The rates of oxygen consumption at high and low alanine concentrations appear to be independent of the oxygen concentration (data not shown), consistent with a K_{O2} value of less than 25 μM. The low K_{O2} value allows for the determination of k_{cat} and k_{cat}/K_{ala} under ambient oxygen concentrations. To determine if the reaction follows pathway a or b in Scheme 2, rates of oxygen consumption were determined in the presence and in the absence of catalase. The presence of catalase slowed the reaction by a factor of 2.2 $\pm$ 0.1, consistent with a stoichiometric amount of hydrogen peroxide being released per oxygen consumed. Moreover, HPLC analyses of alanine oxidation reactions
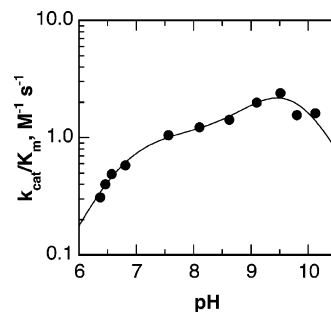

FIGURE 1: pH profiles for alanine oxidation by TMO. The lines are from a fit with eq 1. Assays were done in 0.1 M ACES, 52 mM Tris, 52 mM ethanolamine-HCl, while varying potassium chloride and alanine concentrations to maintain a constant 1.1 M ionic strength at 25 °C. The average error in the data is indicated by the size of the symbols.

showed that pyruvate was the only detectable product, with no evidence for formation of acetamide (results not shown). Thus, TMO is acting as an L-amino acid oxidase with alanine as substrate, following path b in Scheme 2.

pH Effects. The k_{cat} and k_{cat}/K_{ala} values were determined over the pH range 6.4 to 10.1 using a constant ionic strength buffer. Potassium chloride and L-alanine concentrations were varied to maintain a constant ionic strength of 1.1 M. The k_{cat} pH profile was qualitatively similar to the k_{cat} pH profiles for previously characterized amino acid substrates (*31*), with a transition from a low value at pH 6.5 to a higher value above pH 10 (data not shown); however, the increase in K_m values at high pH precluded the accurate determination of k_{cat} values above pH 9.5 and more quantitative analysis of the k_{cat} profile. The k_{cat}/K_m pH profile (Figure 1) is similar to the profiles previously seen for TMO oxidation of other amino acids (*31*). This pH profile was therefore fit to eq 1, which describes a pH dependence with three dissociation constants and plateau regions at both intermediate and high pH. The best fit was obtained by using identical dissociation constants for K_1, which applies to the transition at intermediate pH, and K_3, which applies to the decrease in activity at high pH; the resulting pK_a value of 9.6 $\pm$ 0.1 represents the average of pK_1 and pK_3. Deprotonation of an additional ionizable group with a pK_a value of 6.8 $\pm$ 0.1 (pK_2) was required for activity.

Deuterium Kinetic Isotope Effects. Deuterium kinetic isotope effects were determined by comparing the rates of oxygen consumption using α-protiated and α-deuterated DL-alanine at the pH extremes, 6.5 and 10, and at the intermediate pH region 8.0. The data at pH 6.5 and 8.0 fit best to eq 2, consistent with equal isotope effects on k_{cat} and k_{cat}/K_m.[3] As shown in Table 1, the isotope effects are pH-independent with an average value of 6.0 $\pm$ 0.5. This value is in reasonable agreement with previous studies that showed a $^D(k_{cat}/K_m)$ value of 5.3 $\pm$ 0.5 at pH 8.3 (*31*). The pH-independence of the isotope effect and its equal expression in k_{cat} and k_{cat}/K_m are consistent with irreversible CH bond cleavage and with the observed isotope effect being equal to the intrinsic isotope effect.

Reductive Half-Reaction Kinetics. The reduction of the flavin in TMO by L-alanine was monitored under anaerobic conditions. As shown in Figure 2A, mixing 1 M protiated

---

[3] A $^Dk_{cat}$ value could not be determined at pH 10.0 due to the high alanine concentrations necessary to saturate the enzyme.

Table 1: Deuterium Kinetic Isotope Effects on Alanine Oxidation by TMO

pH	kinetic isotope effect
6.5[a,b]	5.4 ± 0.7
8.0[a,c]	6.6 ± 0.6
10.0[a,c]	6.0 ± 0.3
8.3[d]	6.3 ± 0.9

[a] Determined from steady-state kinetic analysis at 25 °C in air-saturated buffers. [b] 0.1 M ACES, 52 mM Tris, 52 mM ethanolamine-HCl with varied potassium chloride at 1.1 M ionic strength. [c] 0.1 M potassium pyrophosphate. [d] Determined from the rate constants for TMO flavin reduction using 1 M DL-alanine in 50 mM Tris, 5 mM D-glucose, pH 8.3.
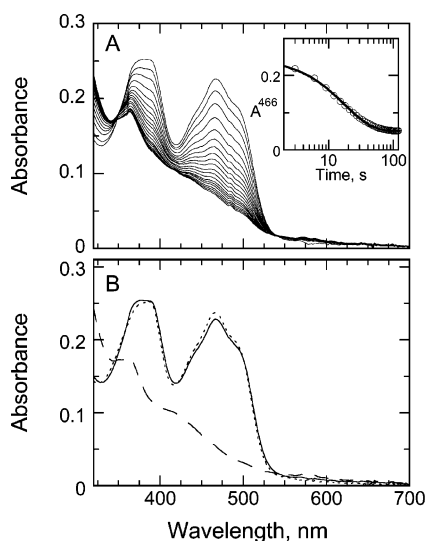

FIGURE 2: Changes in the TMO visible absorbance spectrum during reduction with 1 M L-alanine, pH 8.3. Conditions were as described in Experimental Procedures. (A) The spectra were recorded at 2 s intervals for 40 s. The inset shows the absorbance at 466 nm, measured at 1 s intervals. Every third data point is shown for clarity. The line shows the fit of the data to eq 3, which describes a single-exponential decay. (B) Calculated starting (solid line) and final spectra (dashed line) from a global analysis of the data are compared to the spectrum of free enzyme (dotted line).

L-alanine with enzyme resulted in an isosbestic conversion of fully oxidized to fully reduced flavin. A global analysis of the data from 320 to 800 nm fit well to a single-exponential decay with a rate constant of 0.062 ± 0.001 s^{-1}. Figure 2B shows the starting and final spectra calculated from the global analysis. These spectra are consistent with fully oxidized and reduced flavin, respectively. The similarities between the calculated starting spectrum and the spectrum of free TMO indicates that very little flavin chemistry occurred during the mixing time of the experiment. The absence of any obvious charge-transfer complex in the calculated final spectrum is consistent with a rapid release of product from the reduced enzyme−product complex. As the postulated intermediate flavin species in Schemes 4 and 5 occur prior to CH bond cleavage, reducing flavin with α-deuterated alanine should cause a larger accumulation of either intermediate. The reduction of TMO by 1 M α-^{2}H-alanine was similarly monitored under anaerobic conditions. As with the protiated substrate, the absorbance changes fit best to a single-exponential decay with no indication of an intermediate flavin species. A comparison of the rate constants from the global analyses of flavin reduction using protiated and deuterated alanine gave an isotope effect of
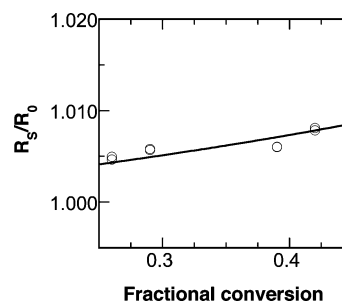

FIGURE 3: Nitrogen isotopic composition of alanine consumption reactions. Samples were analyzed to determine the change in isotopic composition upon oxidation of alanine (R_S/R_0) as described in Experimental Procedures. The line is from the fit of the data to eq 4.

6.3 ± 0.9. This value is in reasonable agreement with the kinetic isotope effects determined under steady-state conditions.

Nitrogen Kinetic Isotope Effects. To determine the ^{15}N kinetic isotope effect on alanine oxidation, L-alanine solutions were oxidized by TMO, yielding a mixture of alanine, pyruvate, and ammonia. As shown by eq 4, calculation of the isotope effect requires an accurate determination of the final percent of alanine consumed (*f*). The relative error in *f* has less impact on the calculated isotope effect as *f* increases. Given the slow nature of both the enzymatic reaction and the rate of diffusion of oxygen into a solution, several days were typically required to achieve a usable percent consumption for alanine. This problem was greatly exacerbated by a time-dependent loss of enzyme activity during turnover. At pH 8.0 and 8.3, it was possible to obtain approximately 25−45% consumption. At higher pH values, the rapid loss of enzymatic activity prevented reactions from reaching a usable percent consumption for alanine. This observation is consistent with a previous analysis of enzyme stability, which showed that TMO is most stable around pH 8 (*27*). After reaching a usable percent consumption, reactions were quenched with acid, and the remaining alanine was isolated and analyzed for its nitrogen isotopic composition. The resulting R_S/R_0 values were analyzed as a function of the percent consumption using eq 4 (Figure 3). The data fit to an observed ^{15}N kinetic isotope effect of 1.0145 ± 0.0007.

Substitution of ^{14}N with ^{15}N raises the pK_a of an amino acid nitrogen, resulting in an isotope effect on the equilibrium between the anionic and zwitterionic forms. This equilibrium isotope effect was determined for the amino acids glycine, alanine, and phenylalanine using ^{13}C NMR. The observed chemical shift of the carboxylate carbon is sensitive to the fractional concentration of the protonated form of the amino acid nitrogen, with an anionic amino acid showing a larger chemical shift relative to its zwitterionic form. At pH values near the amine pK_a, ^{15}N-labeled amino acids will have a slightly larger fractional concentration of the protonated form, resulting in a lower chemical shift. This difference in chemical shifts can be used to calculate the difference in pK_a values between ^{14}N- and ^{15}N-labeled compounds and the resultant equilibrium isotope effect on deprotonation. NMR spectra of samples containing a mixture of ^{14}N- and ^{15}N-labeled compounds were obtained over the pH range 6−13. The difference in the chemical shifts of ^{14}N- and ^{15}N-labeled compounds as a function of the chemical shift of
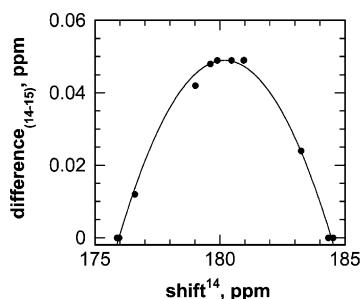
FIGURE 4: Differences in the ^{13}C chemical shifts of the carboxylate carbon for ^{14}N- and ^{15}N-labeled L-alanine as a function of the chemical shift for the ^{14}N-labeled compound. NMR spectra were measured as described in Experimental Procedures. The line is from the fit of the data to eq 5.

Table 2: ^{15}N Equilibrium Isotope Effects on Amino Acid Deprotonation Measured by ^{13}C NMR[a]

amino acid	isotope effect
glycine	1.0226 ± 0.0009
	1.0224 ± 0.0003[b]
	1.0227 ± 0.0002[c]
L-alanine	1.0233 ± 0.0004
L-phenylalanine	1.0229 ± 0.0010

[a] Determined at ambient temperature by ^{13}C NMR using the method of Rabenstein and Mariappan (28), as described in Experimental Procedures. [b] From ref 28. [c] From ref 36.

the ^{14}N-labeled compound are shown in Figure 4 for L-alanine. The isotope effects for deprotonation (Table 2) from fits of the data to eq 5 were essentially identical for all three amino acids, with an average value of 1.0229 ± 0.0004.

DISCUSSION

Tryptophan 2-monooxygenase is the best-studied member of a small class of poorly characterized flavoproteins that catalyze the oxidative decarboxylation of amino acids (32, 33). For TMO, turnover has been shown to proceed through oxidation of the substrate CN bond, yielding an imino acid intermediate (13). Consequently, TMO can be classified as a flavin-dependent amine oxidase, in the same structural family as monoamine oxidase. Like most members of this larger class of enzymes, the chemical mechanism of substrate oxidation by TMO is still controversial. A preliminary characterization of L-alanine oxidation by TMO suggested that CH bond cleavage was rate-limiting for this substrate (31). All of the kinetic data presented here are consistent with this conclusion. Therefore, a more thorough characterization of L-alanine oxidation by TMO allowed the determination of intrinsic isotope effects and provides insight into the chemical mechanism of amine oxidation.

The pH dependence of k_{cat}/K_m shows an ionizable group with a pK_a of 6.8 ± 0.1 that must be deprotonated for activity. A pK_a value of approximately 6.2 was previously measured for the pH dependence of TMO inhibition by competitive inhibitors (31). The reasonable agreement between these two values is consistent with a lack of a forward commitment to catalysis for alanine turnover. The difference in the observed pK_a values can be attributed to an increased stabilization of the positively charged histidinyl residue under the higher ionic strength conditions used for the current study (1.1 vs 0.1 M). Above pH 7, the k_{cat}/K_m values appear to increase in activity upon deprotonation of a second ionizable group

and decrease in activity upon deprotonation of a third ionizable group. A similar k_{cat}/K_m pH profile has previously been described for TMO oxidation of several other amino acids (31); the lower pK_a value was attributed to deprotonation of the amino group of the amino acid substrate (31), while the higher value was later attributed to deprotonation of Tyr413 with a pK_a of 9.8 (17, 31). The average pK_a value of 9.6 ± 0.1 with alanine as substrate is consistent with the alanine pK_a of 9.9 and the tyrosine pK_a, given the increased ionic strength in the present experiments and the lack of a forward commitment to catalysis with alanine.

The observed primary deuterium kinetic isotope effects are pH-independent, with equal values on k_{cat} and k_{cat}/K_m, consistent with the observed value of 6.0 ± 0.5 being the intrinsic value. This conclusion is further supported by the identical isotope effect on the rate constant for flavin reduction. The average value is similar to the intrinsic deuterium kinetic isotope effect of 5.7 for D-amino acid oxidase with D-alanine as substrate (34), despite the differences in stereochemistry and overall protein structure.

The culmination of several decades of study has led to the general consensus that D-amino acid oxidase utilizes a hydride transfer mechanism for substrate oxidation (see ref 26 for a recent review). However, the mechanisms of other flavin-dependent amine oxidases are still debated. With the exception of a hydride transfer, the proposed mechanisms, represented by Schemes 4 and 5, require an intermediate flavin species between fully oxidized and fully reduced flavin for which there is no spectroscopic evidence. For TMO oxidation of L-alanine, the observed deuterium kinetic isotope effects rule out the rate-limiting formation of an intermediate in which the CH bond is intact. Furthermore, as CH bond cleavage occurs approximately 6-fold slower with α-deuterated alanine than with the protiated substrate, reduction with this slower substrate should result in a comparable increase in the accumulation of any preceding intermediates. No such intermediate is seen. Although this observation is insufficient to rule out the above proposed mechanisms,[4] the simplest explanation for the lack of a detectable intermediate flavin species is a mechanism that does not form any intermediate flavin species, i.e., a hydride transfer mechanism.

Heavy atom isotope effects can be used to further address this and other mechanistic possibilities for TMO. The ^{15}N kinetic isotope effects on k_{cat}/K_m report on changes in the alanine nitrogen's bonding order that occur prior to or during the first irreversible step in oxidation. The observed deuterium kinetic isotope effects are consistent with an irreversible CH bond cleavage. Therefore, the ^{15}N kinetic isotope effects also report on the relative timing of changes in the nitrogen bond order and CH bond cleavage. Oxidation of L-alanine by TMO has an isotope effect of 1.0145 ± 0.0007 at pH 8. This value is in agreement with the value of 1.013 previously

---

[4] Although the lack of an observed intermediate is insufficient to rule out its formation, this observation does provide an upper limit for the amount of enzyme flavin that may accumulate in any postulated intermediate form. As previously argued for the flavoenzyme N-methyltryptophan oxidase (2), if one assumes that any flavin intermediate that accumulates to 35% would be detected, the lack of a detectable intermediate during flavin reduction with the deuterated substrate places an upper limit of 6% on the amount of enzyme that accumulates in this form prior to CH bond cleavage.

measured for D-serine oxidation by D-amino acid oxidase at pH 7.5 (*35*), further suggesting that both enzymes utilize a similar chemical mechanism.

Regardless of the mechanism of amino acid oxidation, a proton must be removed from the substrate nitrogen to form the imino acid product. Therefore, the observed $^{15}k_{cat}/K_m$ value at neutral pH is a product of the equilibrium isotope effect on deprotonation of the substrate amine ($^{15}K_{eq}$) and the pH-independent isotope effect on nitrogen rehybridization during CH bond cleavage ($^{15}k_{chem}$). The ^{15}N equilibrium isotope effect of 1.0233 measured for the deprotonation of L-alanine by NMR is identical with values for deprotonation of glycine reported previously (*28*, *36*) and in the present work and for the present value for phenylalanine. The agreement between all three measured values suggests that a similar isotope effect may be seen for the deprotonation of any amino acid with a non-charged side chain.[5] Separation of the equilibrium isotope effect for deprotonation and the isotope effect on rehybridization using eq 6 yields a $^{15}k_{chem}$ value of 0.9917 ± 0.0006.[6] This value can be used to evaluate the proposed chemical mechanisms.

Miller and Edmondson have proposed the involvement of a covalent substrate-flavin adduct for monoamine oxidase (*37*) as one alternative to a hydride transfer mechanism for the oxidation of amines by flavoenzymes. This mechanism, shown in Scheme 4 for TMO oxidation of alanine, involves a nucleophilic attack of the alanine nitrogen on the flavin cofactor. As the alanine attacks the flavin C4a, the increase in electron density at N5 would result in the formation of a strong base with a pK_a value of approximately 30 (*37*), equivalent to that of an amino acid α-carbon (*38*). Thus, formation of the adduct is concerted with cleavage of the alanine CH bond. This mechanism is consistent with the lack of detectable flavin intermediates for TMO oxidation of alanine, as the postulated intermediate is formed during the rate-limiting step. However, it is not consistent with the observed ^{15}N kinetic isotope effects. As previously mentioned, $^{15}(k_{cat}/K_m)$ values report on changes that occur prior to or during the first irreversible step. For the mechanism of Scheme 4, formation of the flavin adduct is concerted with CH bond cleavage and therefore irreversible; subsequent steps do not contribute to the observed $^{15}(k_{cat}/K_m)$ values. Adduct formation involves formation of a fourth bond to the deprotonated alanine nitrogen without changing the nitrogen's hybridization. This reaction is analogous to protonating the amine. The equilibrium kinetic isotope effect for protonation of the amine is simply the reciprocal of the equilibrium effect for deprotonation of the amine. Therefore, the observed isotope effect should equal 1.00 at pH 8 and have a $^{15}k_{chem}$ value of 0.978. Alternatively, formation of the

Scheme 6
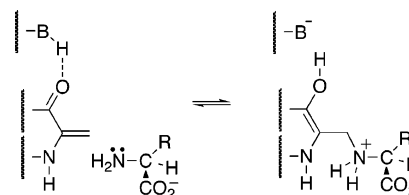
Scheme 7
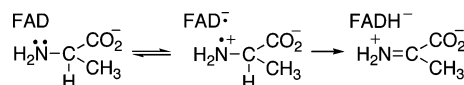
covalent adduct can be compared to the nucleophilic attack of phenylalanine on the enzyme cofactor in phenylalanine ammonia-lyase (Scheme 6), for which a pH-independent ^{15}N kinetic isotope effect of approximately 0.98 was previously measured (*4*). These estimated ^{15}N isotope effects are much more inverse than the observed value of 0.9917. This suggests that TMO does not use the proposed nucleophilic attack mechanism.

In addition to the mechanisms of Schemes 3 and 4, mechanisms involving single electron transfers are often proposed for flavin-dependent amine oxidations (*25*). These mechanisms start with the formation of an anionic flavin semiquinone and a substrate aminium radical, which can then be resolved through a stepwise proton and electron transfer (Scheme 5) or through the direct transfer of a hydrogen atom (Scheme 7). For the mechanism of Scheme 5, CH bond cleavage is concerted with rehybridization of the substrate aminium radical to an sp^3 hybridization for the nitrogen. As this is the first irreversible step, the $^{15}(k_{cat}/K_m)$ values for this mechanism report on the formation of the alanine α-carbon radical from free alanine. The nitrogen bonding order is essentially identical for this radical and the unprotonated free alanine. The $^{15}k_{chem}$ value for this mechanism is not expected to differ significantly from unity,[7] so that the observed isotope effect at pH 8.0 would be approximately 1.023. This mechanism is therefore inconsistent with the observed ^{15}N kinetic isotope effects.

In Scheme 7, CH bond cleavage is concerted with rehybridization of the aminium radical to form the Schiff base product. The $^{15}(k_{cat}/K_m)$ values for this mechanism report on the same net reaction as for a hydride transfer mechanism. This mechanism is therefore consistent with the observed ^{15}N isotope effects. However, as discussed above, the lack of a detectable flavin intermediate does not support this mechanism. Moreover, energetic arguments have previously been raised against formation of the initial radical pair. Walker and Edmondson (*39*) argue that flavoenzymes, whose reduction potentials are typically less than 0.2 V vs SHE,[8] are unlikely to catalyze the one electron oxidation of primary amines, which have estimated reduction potentials well above

---

[5] The values presented are all higher than the previously reported value for amino acid deprotonation of 1.0167 (*3*). The reason for the differences is not clear. The previously reported value was calculated from the equilibrium isotope effects on three different chemical reactions (*4*). In contrast, the values reported here were determined directly from the differences in the equilibrium constants for the ^{14}N- and ^{15}N-labeled compounds.

[6] The reported value does not account for one of the four reactions being run at pH 8.3 instead of pH 8.0. This difference can be accounted for by combining eqs 4 and 6 and fitting the observed R_S/R_0 values simultaneously as a function of both f and pH. This analysis yields a value of 0.9918 ± 0.0006. As the two values are indistinguishable, the simpler analysis was used.

---

[7] The equilibrium ^{15}N isotope effect for formation of the amino acid radical in Scheme 5 was calculated at the B3-LYP level with the 6-311+G** basis set to be 1.0015, using the programs Gaussian 94 (*5*) and QUIVER (*6*). (Kurtz, K. A., and Fitzpatrick, P. F., unpublished results).

[8] Values as large as 230 and approximately 300 mV have been reported for trimethylamine dehydrogenase (*7*) and monoamine oxidase (*8*), respectively. However, the conclusion of the presented argument remains unchanged even with these more favorable reduction potentials.

1 V vs SHE.[9] In light of these arguments, the simplest conclusion is that TMO does not utilize any of the currently proposed single electron-transfer mechanisms.

The lack of visible flavin intermediates during anaerobic flavin reduction, the fully expressed deuterium and nitrogen kinetic isotope effects, and the predicted symmetrical transition state are all consistent with a hydride transfer mechanism for amine oxidation by tryptophan 2-monooxygenase. Currently, D-amino acid oxidase is the only other flavin-dependent amine oxidase for which deuterium and nitrogen kinetic isotope effect data are available (*26*). As discussed above, the similarity between the observed isotope effects is consistent with similar mechanisms for alanine oxidation by these two enzymes; D-amino acid oxidase is accepted to utilize a hydride transfer mechanism (*26*). D-Amino acid oxidase and tryptophan 2-monooxygenase represent the two different structural families of flavin-dependent amine oxidases. These results therefore add to the growing body of evidence that a hydride transfer mechanism is common among all flavin-dependent amine oxidases.

ACKNOWLEDGMENT

REFERENCES

1. Cleland, W. W. (2005) The use of isotope effects to determine enzyme mechanisms. *Arch. Biochem. Biophys. 433*, 2−12.

2. Ralph, E. C., and Fitzpatrick, P. F. (2005) pH and kinetic isotope effects on sarcosine oxidation by N-methyltryptophan oxidase. *Biochemistry 44*, 3074−3081.

3. Rishavy, M. A., and Cleland, W. W. (1999) ^{13}C, ^{15}N, and ^{18}O equilibrim isotope effects and fractionation factors. *Can. J. Chem. 77*, 967−977.

4. Hermes, J. D., Weiss, P. M., and Cleland, W. W. (1985) Use of nitrogen-15 and deuterium isotope effects to determine the chemical mechanism of phenylalanine ammonia-lyase. *Biochemistry 24*, 2959−2967.

5. Frisch, M. J., Trucks, G. W., Schlegel, H. B., Gill, P. M. W., Johnson, B. G., Robb, M. A., Cheeseman, J. R., Keith, T., Petersson, G. A., Montgomery, J. A., Raghavachari, K., Al-Laham, M. A., Zakrzewski, V. G., Ortiz, J. V., Foresman, J. B., Cioslowski, J., Stefanov, B. B., Nanayakkara, A., Challacombe, M., Peng, C. Y., Ayala, P. Y., Chen, W., Wong, M. W., Andres, J. L., Replogle, E. S., Gomperts, R., Martin, R. L., Fox, D. J., Binkley, J. S., Defrees, D. J., Baker, J., Stewart, J. P., Head-Gordon, M., Gonzalez, C., and Pople, J. A. (1995), Gaussian, Inc., Pittsburg, PA.

6. Saunders, M., Laidig, K. E., and Wolfsberg, M. J. (1989) Theoretical calculation of equilibrium isotope effects using ab initio force constants: application to NMR isotopic perturbation studies. *J. Am. Chem. Soc. 111*, 8989−8994.

7. Pace, C. P., and Stankovich, M. T. (1991) Oxidation-reduction properties of trimethylamine dehydrogenase: effect of inhibitor binding. *Arch. Biochem. Biophys. 287*, 97−104.

8. Sablin, S. O., and Ramsay, R. R. (2001) Substrates but not inhibitors alter the redox potentials of monoamine oxidases. *Antioxid. Redox Signal. 3*, 723−729.

9. Alfassi, Z. (1999) *S-Centered Radicals*; Wiley: Chichester; New York.

10. Comai, L., and Kosuge, T. (1980) Involvement of plasmid deoxyribonucleic acid in indoleacetic acid synthesis in *Pseudomonas savastanoi. J. Bacteriol. 143*, 950−957.

11. Comai, L., and Kosuge, T. (1982) Cloning and characterization of *iaaM*, a virulence determinant of *Pseudomonas savastanoi. J. Bacteriol. 149*, 40−46.

12. Klee, H., Montoya, A., Horodyski, F., Lichtenstein, C., Garfinkel, D., Fuller, S., Flores, C., Peschon, J., Nester, E., and Gordon, M. (1984) Nucleotide sequence of the tms genes of the pTiA6NC octopine Ti plasmid: Two gene products involved in plant tumorigenesis (*Agrobacterium tumefaciens*). *Proc. Natl. Acad. Sci. U.S.A. 81*, 1728−1732.

13. Emanuele, J. J., Jr., and Fitzpatrick, P. F. (1995) Mechanistic studies of the flavoprotein tryptophan 2-monooxygenase. 1. Kinetic mechanism. *Biochemistry 34*, 3710−3715.

14. Eberlein, G., and Bruice, T. C. (1983) The chemistry of a 1,5-diblocked flavin. 2. Proton and electron transfer steps in the reaction of dihydroflavins with oxygen. *J. Am. Chem. Soc. 105*, 6685−6697.

15. Lockridge, O., Massey, V., and Sullivan, P. A. (1972) Mechanism of action of the flavoenzyme lactate oxidase. *J. Biol. Chem. 247*, 8097−8106.

16. Sobrado, P., and Fitzpatrick, P. F. (2003) Analysis of the role of the active site residue Arg98 in the flavoprotein tryptophan 2-monooxygenase, a member of the L-amino oxidase family. *Biochemistry 42*, 13826−13832.

17. Sobrado, P., and Fitzpatrick, P. F. (2003) Identification of Tyr413 as an active site residue in the flavoprotein tryptophan 2-monooxygenase and analysis of its contribution to catalysis. *Biochemistry 42*, 13833−13838.

18. Mattevi, A., Vanoni, M. A., Todone, F., Rizzi, M., Teplyakov, A., Coda, A., Bolognesi, M., and Curti, B. (1996) Crystal structure of D-amino acid oxidase: A case of active site mirror-image convergent evolution with flavocytochrome b_2. *Proc. Natl. Acad. Sci. U.S.A. 93*, 7496−7501.

19. Trickey, P., Wagner, M. A., Jorns, M. S., and Mathews, F. S. (1999) Monomeric sarcosine oxidase: structure of a covalently flavinylated amine oxidizing enzyme. *Structure 7*, 331−345.

20. Settembre, E. C., Dorrestein, P. C., Park, J., Augustine, A. M., Begley, T. P., and Ealick, S. E. (2003) Structural and mechanistic studies on *thiO*, a glycine oxidase essential for thiamin biosynthesis in *Bacillus subtilis. Biochemistry 42*, 2971−2981.

21. Binda, C., Newton-Vinson, P., Hubalek, F., Edmondson, D. E., and Mattevi, A. (2002) Structure of human monoamine oxidase B, a drug target for the treatment of neurological disorders. *Nat. Struct. Biol. 9*, 22−26.

22. Binda, C., Coda, A., Angelini, R., Federico, R., Ascenzi, P., and Mattevi, A. (1999) A 30 Å long U-shaped catalytic tunnel in the crystal structure of polyamine oxidase. *Structure 7*, 265−276.

23. Pawelek, P. D., Cheah, J., Coulombe, R., Macheroux, P., Ghisla, S., and Vrielink, A. (2000) The structure of L-amino acid oxidase reveals the substrate trajectory into an enantiomerically conserved active site. *EMBO J. 19*, 4204−4215.

24. Sobrado, P., and Fitzpatrick, P. F. (2002) Analysis of the roles of amino acid residues in the flavoprotein tryptophan 2-monooxygenase modified by 2-oxo-3-pentynoate: characterization of His338, Cys339, and Cys511 mutant enzymes. *Arch. Biochem. Biophys. 402*, 24−30.

25. Scrutton, N. S. (2004) Chemical aspects of amine oxidation by flavoprotein enzymes. *Nat. Prod. Rep. 21*, 722−730.

26. Fitzpatrick, P. F. (2004) Carbanion versus hydride transfer mechanisms in flavoprotein-catalyzed dehydrogenations. *Bioorg. Chem. 32*, 125−139.

27. Emanuele, J. J., Jr., Heasley, C. J., and Fitzpatrick, P. F. (1995) Purification and characterization of the flavoprotein tryptophan 2-monooxygenase expressed at high levels in *E. coli. Arch. Biochem. Biophys. 316*, 241−248.

28. Rabenstein, D. L., and Mariappan, S. V. S. (1993) Determination of ^{15}N isotope effects on the acid-base equilibria of amino groups in amino acids by ^{13}C NMR. *J. Org. Chem. 58*, 4487−4489.

29. Dawson, R. M. C., Elliott, D. C., Elliott, W. H., and Jones, K. M. (1986) *Data for Biochemical Research,* 3rd ed., Clarendon Press, Oxford.

30. Cleland, W. W. (1986) Enzyme kinetics as a tool for determination of enzyme mechanisms, in *Investigation of Rates and Mechanism, 4th Ed., Vol. 6, Part I* (Bernasconi, C. F., Ed.) pp 791−870, John Wiley & Sons, New York.

31. Emanuele, J. J., Jr., and Fitzpatrick, P. F. (1995) Mechanistic studies of the flavoprotein tryptophan 2-monooxygenase. 2. pH and kinetic isotope effects. *Biochemistry 34*, 3716−3723.

32. Flashner, M. I. S., and Massey, V. (1974) Purification and properties of L-lysine monooxygenase from *Pseudomonas fluorescens. J. Biol. Chem. 249*, 2579−2586.

---

[9] One-electron reduction potentials for thiols have been reported in the range of 1.4 V vs SHE (*9*). Replacing sulfur with the more electronegative nitrogen would likely raise this potential.

33. Koyama, H. (1982) Purification and characterization of a novel L-phenylalanine oxidase (deaminating and decarboxylating) from *Pseudomonas sp. P-501*. *J. Biochem. 92*, 1235−1240.

34. Denu, J. M., and Fitzpatrick, P. F. (1994) Intrinsic primary, secondary, and solvent kinetic isotope effects on the reductive half-reaction of D-amino acid oxidase: Evidence against a concerted mechanism. *Biochemistry 33*, 4001−4007.

35. Kurtz, K. A., Rishavy, M. A., Cleland, W. W., and Fitzpatrick, P. F. (2000) Nitrogen isotope effects as probes of the mechanism of D-amino acid oxidase. *J. Am. Chem. Soc. 122*, 12896−12897.

36. Pehk, T., Kiirend, E., Lippmaa, E., Ragnarsson, U., and Grehn, L. (1997) Determination of isotope effects on acid-base equilibria by ^{13}C NMR spectroscopy. *J. Chem. Soc. Perkin Trans. 2*, 445−450.

37. Miller, J. R., and Edmondson, D. E. (1999) Structure-activity relationships in the oxidation of para-substituted benzylamine analogues by recombinant human liver monoamine oxidase A. *Biochemistry 38*, 13670−13683.

38. Rios, A., Amyes, T., and Richard, J. (2000) Formation and stability of organic zwitterions in aqueous solution: enolates of the amino acid glycine and its derivatives. *J. Am. Chem. Soc. 122*, 9373−9385.

39. Walker, M. C., and Edmondson, D. E. (1994) Structure-activity relationships in the oxidation of benzylamine analogues by bovine liver mitochondrial monoamine oxidase B. *Biochemistry 33*, 7088−7098.